

MASSACHUSETTS INSTITUTE OF TECHNOLOGY  
ARTIFICIAL INTELLIGENCE LABORATORY

A.I.Memo 885

May 1987

**Shape from Shading, Occlusion and Texture**

A.L. Yuille

**Abstract:**

Shape from Shading, Occlusion and Texture are three important sources of depth information. We review and summarize work done on these modules.

© Massachusetts Institute of Technology (1987)

This report describes research done within the Artificial Intelligence Laboratory of the Massachusetts Institute of Technology. Support for the laboratory's Artificial Intelligence research is provided in part by the Advanced Research Projects Agency of the Department of Defense under Office of Naval Research contract N00014-85-K-0124 and the System Development Foundation.

## 1. Introduction

Vision is a highly complex process. There is an important distinction between those visual processes which involve high level, or semantic, information and *early vision* processes which do not use such knowledge. A primary goal of an early vision system, be it human or mechanical, is to determine and represent the shape of objects from their image intensities. Marr (1982) calls such a representation, which makes explicit the distance to, and orientation of, the visible surfaces from the standpoint of the viewer, a  $2 - 1/2D$  sketch. He describes several independent processes, or *modules*, which compute it. Marr's research focussed on stereopsis and structure from motion. In this chapter we will consider other modules: shape from shading, shape from occlusion boundaries and shape from texture.

The image intensities are the basic inputs to any vision system. For a camera they consist of an array of numbers measured by electronic sensors. In the human eye these measurements are made by a million neurons that undergo chemical changes in response to light. Unlike stereopsis, shape from shading calculates the shape of a surface from a single image. People can estimate the shape of a face from a single photograph in a magazine. This suggests that there is enough information in one image, or at least that we make additional assumptions. The key point is that because different parts

of the surface are oriented differently they appear with different brightnesses and this can be employed to estimate the surface orientation. By itself this only provides one constraint for the two degrees of freedom of orientation. Additional assumptions, such as surface smoothness, are needed.

The light intensity that enters our eyes, or a camera lens, is not directly related to the structure of the objects being viewed. It depends on the strength and positions of the light sources and the reflectance functions of the objects. The reflectance function of an object determines how much light the object reflects in any given direction. In pioneering work, Horn (1970, 1975) showed how to determine shape from shading by modelling the image formation process with the image irradiance equation. In this equation the reflectance functions of objects are written in a simple mathematical form. It is possible to invert this equation and estimate the shape of the object, provided the position of the light source and the reflectance function of the object are known. For this solution to be unique, one needs additional constraints, such as the directions of the surface normals on the boundary of the object. These constraints can be imposed as boundary conditions on the image irradiance equation.

There are two types of object boundaries. The first is due to a discontinuity in the surface normal, such as the boundary of a knife blade. The

second occurs when the surface turns smoothly away from the viewer and is called an *occlusion* boundary (see figure 1.). It is possible to get a surprising amount of information about an object's shape from occlusion boundaries. This knowledge can be used as boundary conditions for a shape from shading process. It can also strongly constrain the geometrical structure of the object being viewed.

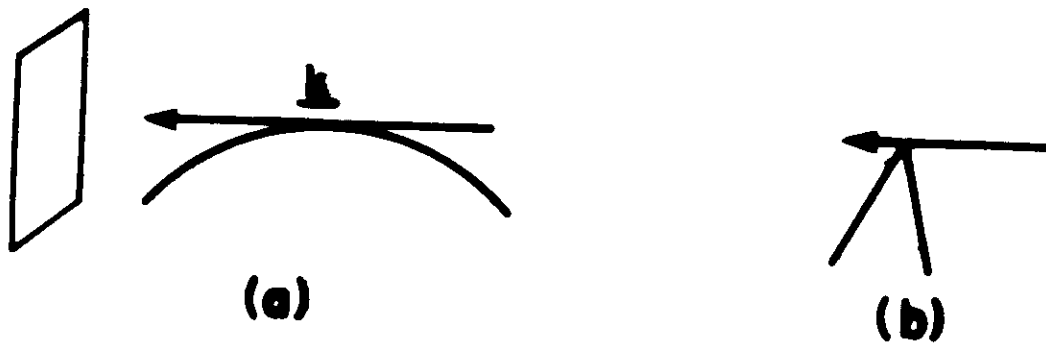


*Figure 1(a) shows an occluding boundary where the light ray grazes the surface. Figure (b) shows a discontinuity boundary.*

Another source of depth information is texture. Gibson (1950) observed that textured objects with repeating patterns can give a strong impression of depth. This effect has often been exploited by artists. In the final section we briefly review work on this module.

## 2. Setting up Shape from Shading

The human visual system has a weak ability to use shading information to determine shape. A common example of this is the use of make-up in everyday life which can have dramatic effects when skillfully applied. It seems unlikely, however, that this ability is highly developed. In most natural situations the lighting conditions are too complicated and the reflectance properties of the objects are too varied. Furthermore the existing psychophysical evidence, though limited, suggests that the information it yields is weak.

Nonetheless shape from shading is one of the most analysed visual modules. Horn (1975) derived a differential equation, the *image irradiance equation*, relating the image intensity to the surface orientation. He assumed the illumination was simple and the surface reflectance was known. These assumptions limit the domain of this approach. It is impractical to solve these equations for complex lighting situations, such as most indoor scenes, where there is mutual reflectance between objects and many light sources. They are most useful for situations where the lighting can be modelled by a point source and a diffuse component, such as aerial photography, or in industrial applications where the lighting can be controlled. Horn and Ikeuchi (Ikeuchi et al 1984, Horn and Ikeuchi 1984) describe how shape from shading can enable a robot to identify an object and extract it from a bin of parts.

The basic geometry of the situation is shown in figure 2. The fraction of light reflected from an object depends on the structure of the object and can usually be described as a function of the directions of the viewer  $\vec{k}$ , source  $\vec{s}$  and surface orientation  $\vec{n}$ . Let  $i, e, g$  be the angles between  $\vec{n}$  and  $\vec{s}$ ,  $\vec{n}$  and  $\vec{k}$ , and  $\vec{k}$  and  $\vec{s}$ . Let  $\vec{x}$  be the position of the point in the image. The reflection of light by the surface can be described by the *image irradiance equation*

$$E(\vec{x}) = R(\vec{k}, \vec{s}, \vec{n}) \quad (2.1)$$

where  $E(\vec{x})$  is the image intensity grey level measured by the viewer at point  $\vec{x}$  and  $R$  is the reflectance function of the object. Many surfaces can be modelled as combinations of Lambertian and specular surfaces. Lambertian, or pure matte, surfaces look equally bright from all directions. Their reflectance function  $R_L$  is just the cosine of the angle between the light source and the surface normal and can be written

$$R_L = \vec{s} \cdot \vec{n} = \cos(i). \quad (2.2)$$

The ideal specular surface is a mirror. The reflectance function  $R_S$  is 1 if  $\vec{s}$ ,  $\vec{n}$  and  $\vec{k}$  are coplanar and  $\vec{s} \cdot \vec{n} = \vec{k} \cdot \vec{n}$ \*, and 0 otherwise. However most specularities in the real world is not pointlike and extensions are needed. One

---

\*Equivalently  $i = e$  and  $g = i + e$ .

model smoothes  $R_S$  by convolving it with a gaussian. Another approach is taken by Computer Graphics models. Let  $\vec{h}$  be the unit vector bisecting  $\vec{s}$  and  $\vec{k}$  as in figure 2. Then perfect specular reflection will only occur when  $\vec{n} \cdot \vec{h} = 1$ . So to model specularity we can use a reflectance function  $R_S = (\vec{h} \cdot \vec{n})^m$  where  $m$  is a large number, often  $m = 16$ . This function has a single maximum at points where  $\vec{n} \cdot \vec{h} = 1$  and then falls off sharply. The speed of the fall off increases as  $n$  increases.

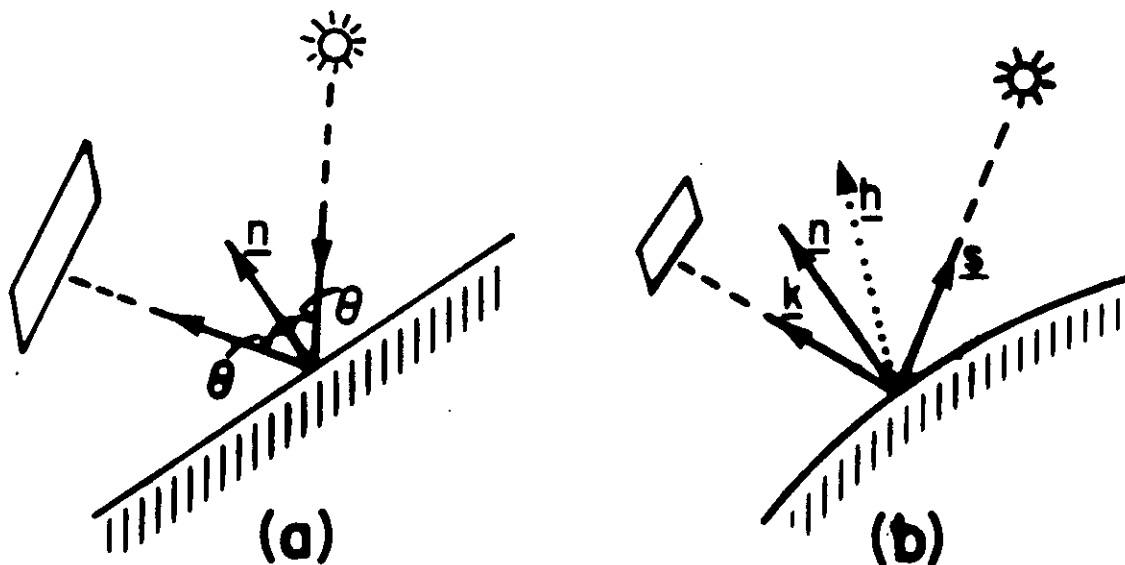


Figure 2(a) shows a light ray being reflected by an ideal mirror. In figure (b) the specular reflectance is a function of  $\vec{n} \cdot \vec{h}$ .

Horn (1979) gives examples of many different types of reflectance function. For instance, for fixed  $g$ , the rocky surface of the maria of the moon can be modelled by  $R_M$  where

$$R_M = \frac{\cos(i)}{\cos(e)}. \quad (2.3)$$

This has the interesting property that if the source of illumination is directly behind the viewer, so that  $i = e$ , the surface will be of constant brightness. This effect is easily observed when the sun, earth and moon are appropriately aligned.

A crucial problem for shape from shading concerns the uniqueness of the solution. Even if the light source direction is known there is one equation for two unknowns, the two independent coefficients of the surface normal, at each point. Thus simple number counting suggests that more information is needed to guarantee uniqueness. Uniqueness results are discussed further in section 5.

There have been disappointingly few psychophysical experiments investigating shape from shading. In recent work Todd and Mingolla (1983) displayed the images of cylindrical surfaces of different radii and asked subjects to estimate the curvature. They showed that humans were able to get a weak estimate of the surface shape and were better at finding the light source direction. Adding some texture patterns, to allow shape from texture, improved their performance. Specular highlights did not seem to influence these results. This work is very preliminary and more research is needed in this area.



It has been found empirically (Woodham 1980) that the Lambertian is a surprisingly good model for many aerial photographs. However there are a number of atmospheric effects (Sjoberg 1982) which must be taken into account. A recent report (Woodham and Lee 1984) concludes that atmospheric effects, such as the scattering of the direct solar beam, are important and vary locally with elevation. The sky irradiance is also significant and must be modelled explicitly.

### 3. Gradient space and characteristic strips

An important issue for all vision problems is the choice of representation. Workers in shape from shading have often used a representation for surfaces known as Gradient space. This was developed by Huffman (1971) and Mackworth (1973) in another context. It was first used for shape from shading by Horn (1977).

We choose a coordinate system such that the image lies in the  $x,y$  plane. An arbitrary point on a surface  $z = f(x, y)$  is given by

$$\vec{r} = (x, y, f(x, y)). \quad (3.1)$$

The surface normal is

$$\vec{n} = \frac{1}{(1 + f_x^2 + f_y^2)^{1/2}}(-f_x, -f_y, 1), \quad (3.2)$$

where  $f_x$  and  $f_y$  are the partial derivatives of  $f$  with respect to  $x$  and  $y$ . They can be denoted by  $p$  and  $q$  respectively. The coordinate frame based on  $(p, q)$  is *Gradient space*. In this space a planar surface  $ax + by + c = z$  is represented by a point  $p = a, q = b$  (see figure 3.). Using this notation the image irradiance equation (Horn 1977) becomes

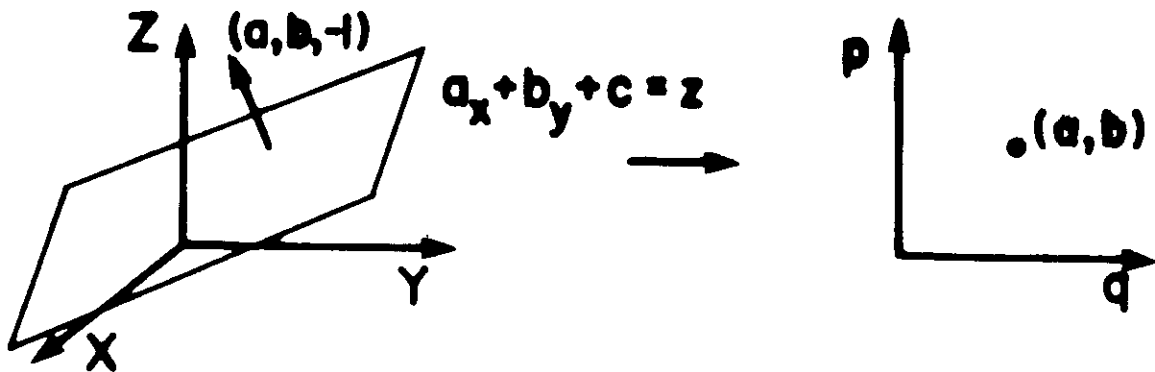
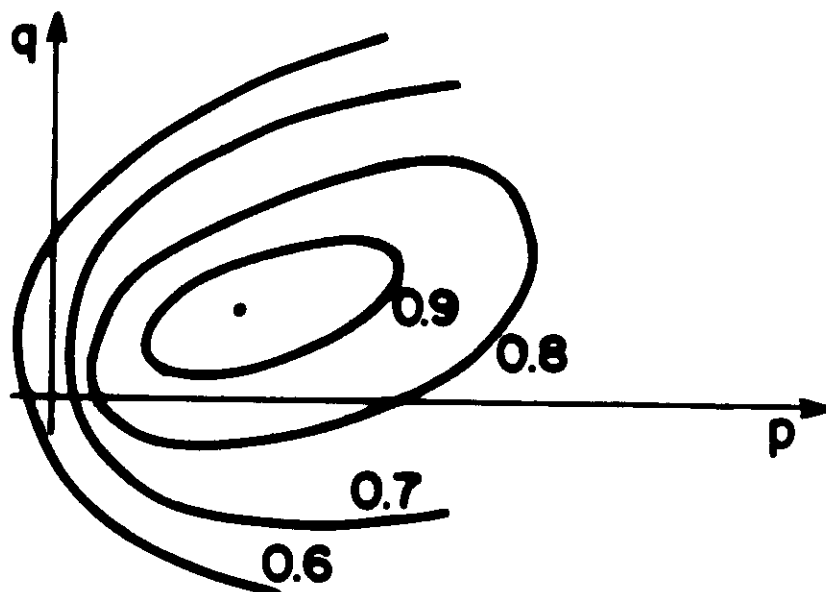


Figure 3. A plane  $ax + by + c = z$  is represented by a point  $(a, b)$  in Gradient space.

$$E(x, y) = R(p, q). \quad (3.3)$$

The problem now is to recover the surface  $z = f(x, y)$  given the image

intensity  $E(x, y)$  and the form of the reflectance function  $R$ . Figure 5 shows contours of constant intensity as a function of  $p$  and  $q$  for a specific reflectance function. Many reflectance functions can be expressed simply in terms of Gradient space. For example it is easy to verify that the reflectance function of the maria of the moon  $R_M$ , given by (3.3), is a linear combination of  $p$  and  $q$ .



*Figure 4. Contours of constant intensity in Gradient space.*

Gradient Space has a serious disadvantage which we will discuss in more detail in section 4. At occluding boundaries both  $f_x$  and  $f_y$  become infinite and so  $p$  and  $q$  are undefined although the surface normal is well behaved. Thus the coordinate system breaks down at occluding boundaries. These boundaries are often important as boundary conditions for variational shape

from shading.

The image irradiance equation (3.3) is a non-linear, first-order partial differential equation. Horn (1975) applies the characteristic strip method to reformulate the problem. This is illustrated in figure 5. Suppose we know  $(p, q)$  at a point on the surface. We can define the characteristic strip curve  $(x(s), y(s), z(s))$  by

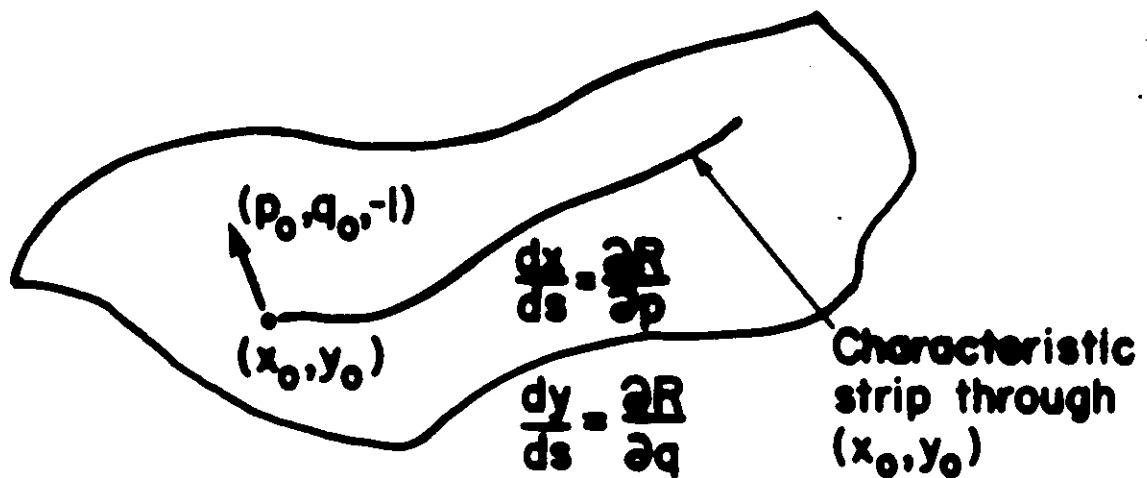


Figure 5. The characteristic strip through  $(x_0, y_0)$ . Its tangent direction, in the  $(x, y)$  plane,  $(dx/ds, dy/ds)$  is along the gradient of the Reflectance function in Gradient space  $(\partial R/\partial p, \partial R/\partial q)$ .

$$\frac{dx}{ds} = \frac{\partial R}{\partial p}, \quad (3.4a)$$

$$\frac{dy}{ds} = \frac{\partial R}{\partial q}, \quad (3.4b)$$

$$\frac{dz}{ds} = p \frac{\partial R}{\partial p} + q \frac{\partial R}{\partial q}. \quad (3.4c)$$

Note that the dot product of the tangent to this curve with the surface normal  $\vec{n}$ , given by (3.2), is zero. Thus the curve lies on the surface. In terms of  $p$  and  $q$  this becomes

$$p \frac{dx}{ds} + q \frac{dy}{ds} - \frac{dz}{ds} = 0. \quad (3.5)$$

Differentiating eq. (3.3) with respect to  $x$  gives

$$E_x = R_p p_x + R_q q_x. \quad (3.6)$$

Since  $p_y = f_{xy} = q_x$  we find

$$E_x = R_p p_x + R_q p_y \quad (3.7)$$

and so, using eq. (3.4), we get

$$E_x = \frac{dp}{ds}. \quad (3.8)$$

Similarly

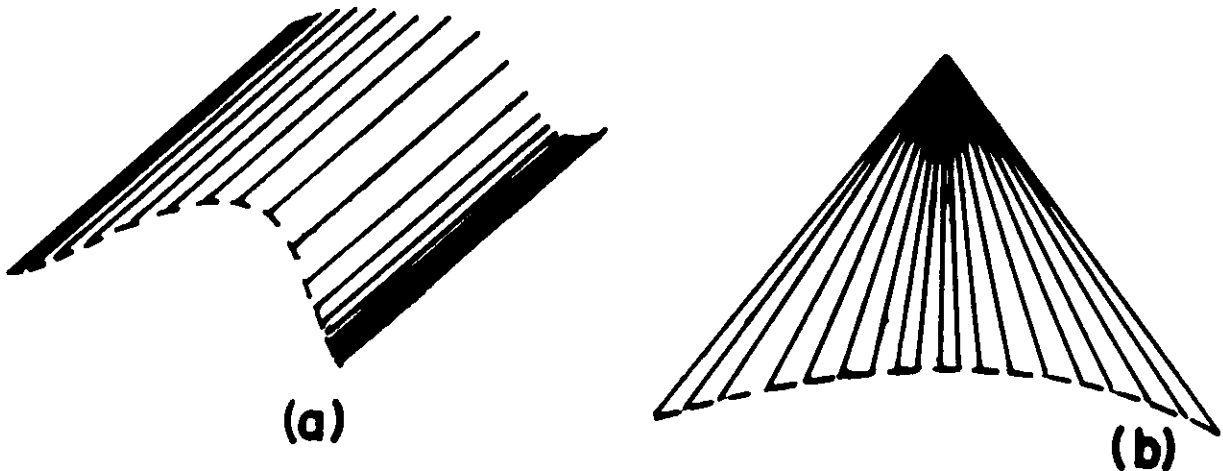
$$E_y = \frac{dq}{ds}. \quad (3.9)$$

These equations can be used (Horn 1975) as a basis for an iterative computation. Suppose the surface gradient  $(p_0, q_0)$  is known at a point  $(x_0, y_0)$ . We can find the tangent to the characteristic strip at this point from eq. (3.4). Using the intensity gradient we can use (3.8) and (3.9) to calculate  $dp/ds$  and  $dq/ds$ . Thus we can determine the gradient  $(p_1, q_1)$  at  $(x_1, y_1)$ . Repeating this procedure we can calculate  $p$  and  $q$  along the characteristic strip curve. The set of all characteristic strips will span the surface. So if we know the surface normal on one point on each characteristic strip we can use this method to recover the surface.

The characteristic strip method has several disadvantages. It needs the surface at the initial point to be convex, it is complex to compute and it is very susceptible to noise. In addition the surface normal at the initial point for each characteristic strip must be known. Another problem is the possible non-uniqueness of the inverse shape from shading calculation. It cannot be guaranteed that the strips method will converge to the right answer. From the perspective of human vision the serial nature of the computation makes it biologically implausible.

#### 4. Geometric assumptions and Photometric stereo

An alternative approach to shape from shading is to restrict the surface geometry. The simplest situation is a world of planar surfaces. Horn (1977) showed that if three planes meet at a point then the orientation of the planes can be determined locally by shading information.



*Figures 6(a) and (b) show two developable surfaces.*

Woodham (1981) extends this result to the class of developable surfaces, which includes cylinders and cones. These surfaces are defined so that for every point on the surface there is a straight line ruling through it along which the normal vector is constant, see figure 6. Since the reflection functions depend only on the surface normal the image intensity will therefore be constant along these rulings. Thus it is straightforward to check directly from

the image if a surface is developable. For these surfaces the characteristic strips method, and other more numerically stable techniques, can easily be applied. *Generalized Cylinders* are a class of surfaces much studied in Computer Vision (Binford 1971). They consist of a two-dimensional cross-section which generates a surface as it is moved along a straight axis being allowed to contract or expand provided it keeps the same shape, see figure 7. Woodham (1981) shows how to extend his results to generalized cylinders provided the axis of the cylinder is parallel to the image plane.

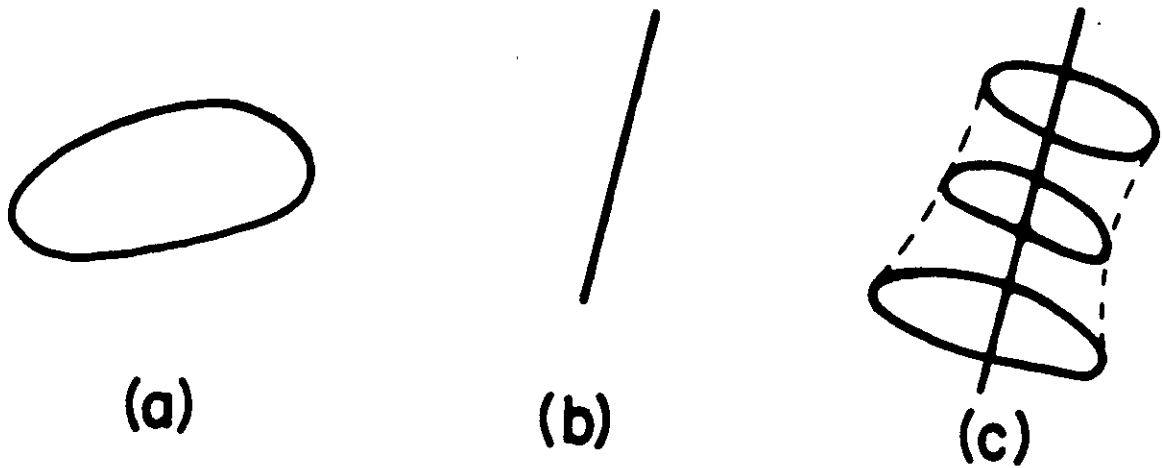


*Figure 7(c) shows a generalized cylinder. Figures (a) and (b) show its cross-section and its axis.*

Pentland (1984) has shown that for Lambertian surfaces at umbilic points, where the principal curvatures of the object are equal, the surface can be de-



terminated locally. This result is limited as the sphere is the only curved surface which is umbilic everywhere and there is no known method of discovering if the surface is umbilic or not. Nevertheless Pentland argues that this requirement can be relaxed and reports good results from this method even when the surface is not umbilic.

Perhaps the most elegant method of using shading information is photometric stereo (Woodham 1978, 1980). Here the direction of incident illumination is varied between two successive views. We denote the two images by  $E_1(x, y)$  and  $E_2(x, y)$  and let the corresponding reflectance functions be  $R_1(p, q)$  and  $R_2(p, q)$ . If the illumination is rotated about the viewing direction then  $R_1$  and  $R_2$  are simply related. The two views yield the equations

$$E_1(x, y) = R_1(p, q) \tag{4.1a}$$

$$E_2(x, y) = R_2(p, q) \tag{4.1b}$$

in the two unknowns  $p$  and  $q$ . These will usually be sufficient to determine the shape. At any point  $(x_1, y_1)$  the first image will constrain  $p$  and  $q$  to lie on the contour  $R_1(p, q) = E_1(x_1, y_1)$  in Gradient Space. Similarly the second image will constrain them to lie on the contour  $R_2(p, q) = E_2(x_1, y_1)$ . These curves will usually intersect in two points allowing at most two consistent surface

gradients. If necessary a third image  $E_3$  could be used.

Photometric stereo can be easily implemented (Silver 1980) and is probably the most practical method of doing shape from shading. It can be speeded up by using a lookup table to attain real-time performance.

## 5. Variational Methods

We mentioned earlier the disadvantages of the characteristic strips approach to solving the image irradiance equation. In this chapter we show how to formulate shape from shading as a minimization problem which can be solved by local parallel processors. These methods are numerically stable and only require a single view. They usually achieve this stability by making smoothness assumptions about the viewed surface. To attain uniqueness they need to know the surface normals on the boundary of the object, see figure 8. For occluding boundaries this information can be found directly from the image (Barrow and Tennenbaum 1981, Ikeuchi 1980). At such boundaries the normals are perpendicular to the projection direction and hence lie perpendicular to the projection of the occluding boundary.

The first parallel scheme was due to Strat (1979). It used the gradients  $p, q$  to express surface orientation and was therefore unable to deal with oc-

cluding boundaries. It was not formulated as a variational problem, but Horn and Brooks (1985) show that it can be expressed in these terms.

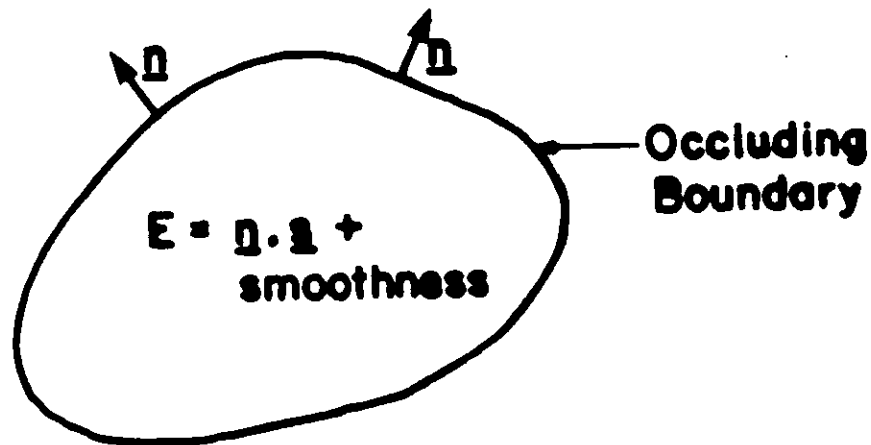


*Figure 8. Variational methods assume knowledge of the normals on the boundaries, the image irradiance equation (Lambertian in this case) and surface smoothness.*

Ikeuchi and Horn (1981) developed another method using the calculus of variations and an alternative coordinate system. In terms of Gradient Space coordinates the surface normal is

$$\vec{n} = \frac{1}{(1 + p^2 + q^2)^{1/2}}(-p, -q, 1), \quad (5.1)$$

At occluding boundaries  $p$  and  $q$  become infinite although the normal itself is well behaved. Ikeuchi and Horn (1981) suggest using coordinates  $f$

and  $g$  given by

$$f = \frac{2p}{1 + (1 + p^2 + q^2)^{1/2}} \quad (5.2a)$$

$$g = \frac{2q}{1 + (1 + p^2 + q^2)^{1/2}}. \quad (5.2b)$$

These coefficients satisfy  $f^2 + g^2 \leq 4$  for all visible parts of a surface. This stereographic space corresponds to projecting the Gaussian sphere of all possible surface orientations onto the plane from its north pole. In contrast gradient space corresponds to a projection from the centre.

In terms of these coordinates the image irradiance equation becomes  $E(x, y) = R(f, g)$ . Let  $\Omega$  be the region on which the image is defined. We define a measure of the brightness error by

$$\int \int_{\Omega} (E(x, y) - R(f(x, y), g(x, y)))^2 dx dy. \quad (5.3)$$

The minimization of the brightness error does not constrain the problem sufficiently. For generic surfaces we expect that neighbouring points will have similar orientations. To impose this Ikeuchi and Horn (1981) add a smoothness term given by

$$\int \int_{\Omega} (f_x^2 + f_y^2 + g_x^2 + g_y^2) dx dy. \quad (5.4)$$

This smoothness term will be small for a surface with few fluctuations in  $f$  and  $g$ . Adding the smoothness error to the brightness error we obtain a functional

$$\int \int_{\Omega} (E(x, y) - R(f(x, y), g(x, y)))^2 + \lambda(f_x^2 + f_y^2 + g_x^2 + g_y^2) dx dy. \quad (5.5)$$

This functional is minimized with respect to  $f$  and  $g$  over the space  $\Omega$ , subject to the boundary conditions.  $\lambda$  is a scalar that assigns a relative weighting to the terms.

It is a standard result of the Calculus of Variations (Courant and Hilbert 1953) that, in most situations, minimizing the functional (5.5) is equivalent to solving the associated Euler-Lagrange equations

$$(E - R)R_f + \lambda \nabla^2 f = 0, \quad (5.6a)$$

$$(E - R)R_g + \lambda \nabla^2 g = 0. \quad (5.6b)$$

Here  $R_f$  and  $R_g$  are the partial derivatives of  $R(f, g)$  with respect to  $f$  and  $g$  and

$$\nabla^2 = \frac{\partial^2}{\partial x^2} + \frac{\partial^2}{\partial y^2} \quad (5.7)$$

is the Laplacian operator. These equations can be solved by a finite difference approach. The Laplacian is written as

$$(\nabla^2 f)_{ij} = \frac{4}{\epsilon^2}(\bar{f}_{ij} - f_{ij}), \quad (5.8)$$

where  $\epsilon$  is the grid spacing and the local average  $\bar{f}_{ij}$  is given by

$$\bar{f}_{ij} = \frac{1}{4}(f_{i,j+1} + f_{i+1,j} + f_{i,j-1} + f_{i-1,j}). \quad (5.9)$$

We can rewrite the Euler-Lagrange equations in this form

$$f_{ij} = \bar{f}_{ij} + \frac{\epsilon^2}{4\lambda}(E_{ij} - R(f_{ij}, g_{ij}))R_f(f_{ij}, g_{ij}), \quad (5.10a)$$

$$g_{ij} = \bar{g}_{ij} + \frac{\epsilon^2}{4\lambda}(E_{ij} - R(f_{ij}, g_{ij}))R_g(f_{ij}, g_{ij}), \quad (5.10b)$$

These equations can be solved using an iterative scheme

$$f_{ij}^{k+1} = \bar{f}_{ij}^k + \frac{\epsilon^2}{4\lambda}(E_{ij} - R(f_{ij}^k, g_{ij}^k))R_f(f_{ij}^k, g_{ij}^k) \quad (5.11a)$$

$$g_{ij}^{k+1} = \bar{g}_{ij}^k + \frac{\epsilon^2}{4\lambda}(E_{ij} - R(f_{ij}^k, g_{ij}^k))R_g(f_{ij}^k, g_{ij}^k) \quad (5.11b)$$

Empirical results demonstrate the effectiveness of this scheme although there is no proof to guarantee that it will converge to the correct solution. The

scheme is intrinsically parallelisable. There are several alternative methods to minimize the cost functional including the gradient descent technique.

The smoothness term is necessary to ensure a well-defined smooth solution. However it does tend to bias the resulting surface. For example if the image corresponds to a sphere the algorithm will yield a distorted sphere. The amount of this distortion depends on the size of the parameter  $\lambda$ . This parameter must be large enough to make the algorithm stable and small enough not to distort the surface too much.

A weakness of this scheme is that it treats  $f$  and  $g$  as being independent variables and makes no use of the integrability constraint (Brooks 1982). This constraint arises because of the "consistency" of the surface and corresponds to the condition  $f_{xy} = f_{yx}$ . In terms of gradient space it is expressed as

$$p_y = q_x. \quad (5.12)$$

We can use (5.2) to write this in terms of  $f, g$  and their derivatives. However it is too complicated to be easily used to constrain the solution.

Strat's method (1979) implicitly uses this constraint although his method is based on an integral form. The scheme can be posed in a functional form (Horn and Brooks 1985) and does not include a smoothing term. Horn and Brooks (1985) describe his work and provide a summary of other work on

variational approaches to shape from shading.

All these approaches assume that the source direction is known accurately, which is unlikely for most realistic situations. To deal with this problem Brooks and Horn (1985) have proposed an iterative scheme using a variational principle that estimates the source direction as it determines the slope. There is no guarantee of convergence of the algorithm but preliminary implementations are encouraging.

## 6. Uniqueness

Bruss (1981) has obtained some results about the uniqueness of the image irradiance equation. She assumes the light source is known and shows that boundary information, usually in terms of occluding contours, is almost always needed. She considers reflectance functions of form  $f(p^2 + q^2)$ , where  $f$  is a one-to-one function. She shows that if the behaviour on the boundary is specified and  $E(x, y)$  has at most one stationary point then the solution is unique up to inversion. A special case of this reflectance function is a Lambertian surface with the light source directly behind, or over the shoulder, of the viewer.

More recently several proofs have been proposed to prove uniqueness for Lambertian surfaces with general viewpoint (Baddoura 1985, Blake 1985b,



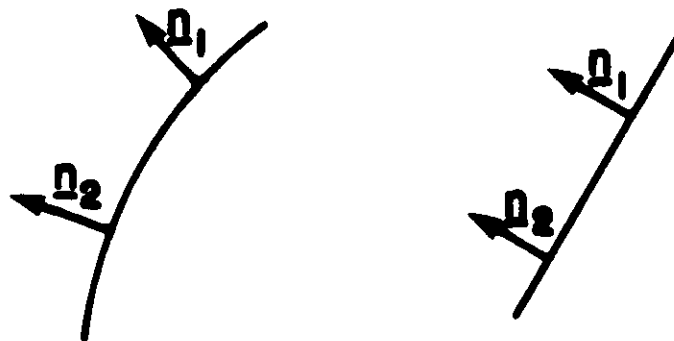
Yuille and Brady 1986) assuming the normal vector on the boundaries is known. Although these proofs are interesting in their own right none of them suggest new algorithms to calculate shape from shading.

If the direction of the light source is unknown there is additional ambiguity (for example see Woodham 1981) and uniqueness results might seem even harder to obtain. Surprisingly this is usually not the case (Yuille and Brady 1986). If the normal to the surface is known then given the form of the reflectance function it is often straightforward to determine its parameters. For example, the Lambertian reflectance function is given by

$$E(x, y) = \vec{s} \cdot \vec{n} \quad (6.1)$$

and is specified by three parameters, the coefficients of  $\vec{s}$ . If the boundary is occluding then the surface normal  $\vec{n}$  is known there. Hence for a typical object there are an infinite number of equations, although they may not be independent, from which to determine  $\vec{s}$ , see figure 9. These may still not give sufficient information as the surface normals at occluding boundaries generally are perpendicular to the viewer direction  $\vec{k}$ . In this case two coefficients of  $\vec{s}$  can be found but the coefficient in the  $\vec{k}$  direction is unknown. Suppose, however, we make the reasonable assumption that there is a point at which the surface normal points directly to the light source. This point can be

easily found since, by (6.1) it will be a global maxima of the image intensity. Moreover the value of the image intensity at that point will be the modulus of  $\vec{s}$ . It is now straightforward to determine the third component of  $\vec{s}$ . This argument does not apply to the example of Woodham (1981) which was a cone and because of its regular structure had no normal pointing towards the light source. This proof can be extended to more general reflectance functions and combinations of them (Yuille and Brady 1986).



*In figure 9(a) there are an infinite number of directions of the surface normal  $\vec{n}$  and hence an infinite number of equations. However if the reflectance is Lambertian there will be only two independent equations. In figure (b) there is only one equation.*

This argument helps for uniqueness proofs but may not yield a stable

method to determine the source direction for real images. Moreover the approximations used to model objects as Lambertian surfaces may not hold near occluding boundaries.

## 7. The Extended Gaussian Image

In order to recognize an object and determine its orientation in space it is necessary to have a way of representing its shape. One such representation which has been proposed by Horn (1982, 1984) is the extended Gaussian Image. Because it explicitly represents shapes by their surface normals it seems particularly appropriate for describing objects found by a module like shape from shading which calculates orientation rather than depth. Each point on the object is represented by a point on the Gaussian sphere corresponding to the direction of the surface normal, see figure 10. If several points on the object have the same surface normal then each such point contributes a unit of "mass". Thus the extended Gaussian sphere representation of an object consists of a mass distribution on the sphere. The total mass of the sphere corresponds to the total surface area of the object. It can be shown that this representation is unique for convex objects. This representation stays invariant under translation of the object and behaves simply under rotation; the

whole sphere rotates by the same amount.

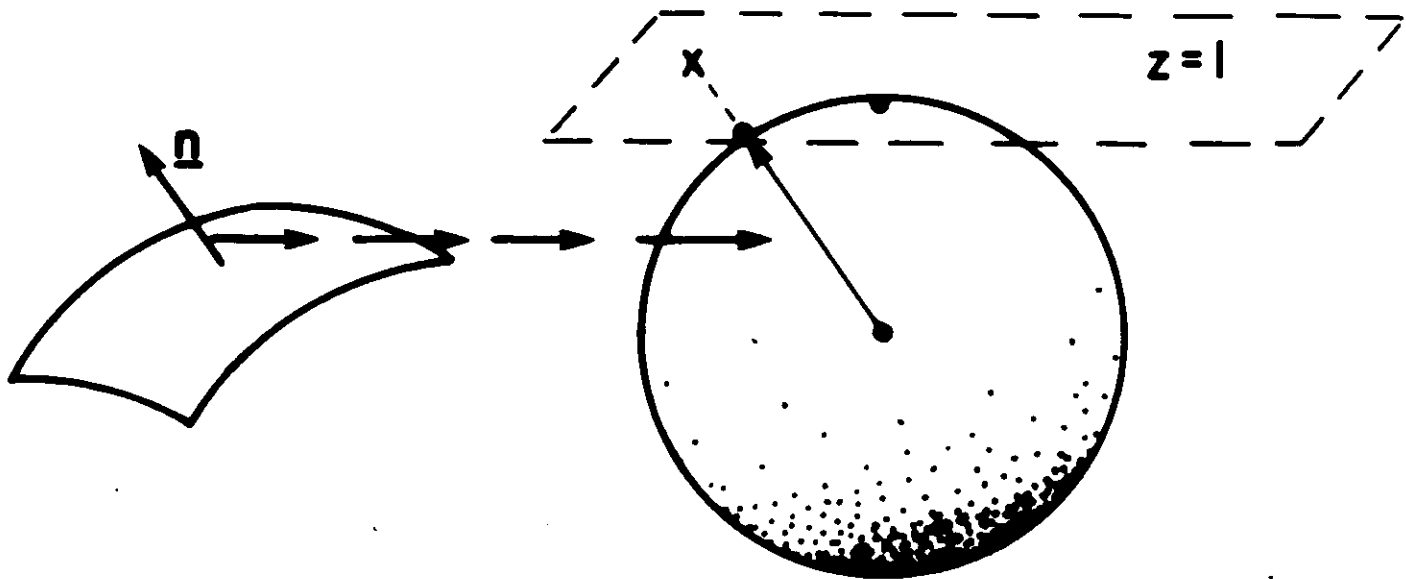


Figure 10. The unit normal to the surface at a point is parallelly transported so that its base lies at the centre of the Gaussian sphere. The point is represented by the position of the tip of the normal on the surface of the sphere. Note that the coordinates of the point in Gradient space are given by the intersection of the line along the normal with the plane  $z = 1$  at the top of the sphere.

## 8. Applications

In this section we discuss two important uses of shape from shading. We first consider using the image irradiance equation to predict the image of a given

screen for aerial photography. Secondly we describe work in which a robot uses shape from shading to pick an object out of a bin of parts.

The study of aerial photographs is a growing application area of shape from shading. For example it is important to monitor areas of harvesting activity. In rugged terrain changes, in image irradiation due to the ground cover are often dominated by changes due to variations in the topography. If the variations in topography can be predicted, then the remaining variations can be interpreted as changes in ground cover and used to determine the state of the harvest. For aerial photography the sun is the unique light source and its exact direction can easily be determined.

The reflectance map can be used to synthesize a model for the variations due to topography. No attempt is made to invert the map. Instead the surface slope information is used as input to the image irradiance equation which then predicts the intensity for a given illuminant and viewer. It is necessary to have good determination of shadow information, which typically correspond to occluding boundaries. For aerial photographs, and Landsat images, the primary light source is the sun and its position must be accurately known at the time that the satellite takes its pictures.

It has been found empirically (Woodham 1980) that the Lambertian is a surprisingly good model for many aerial photographs. However there are a

number of atmospheric effects (Sjoberg 1982) which must be taken into account. A recent report (Woodham and Lee 1984) concludes that atmospheric effects, such as the scattering of the direct solar beam, are important and vary locally with elevation. The sky irradiance is also significant and must be modelled explicitly. This leads to a scene irradiance equation with three terms

$$L_r = \frac{\rho}{\pi} E_e^{-r(z)(1+1/\cos(g))} \cos(i) + \frac{\rho}{\pi} E_{SO} e^{-r(z)} e^{-z/H_s} \frac{(1 + \cos(e))}{2} + L_{PO} e^{-z/H} \quad (8.1)$$

where  $r(z) = r e^{-z/H}$ . These three terms correspond to solar irradiance, sky irradiance and path radiance respectively.  $E$ ,  $\rho$ ,  $r$ ,  $E_{SO}$ ,  $H_s$ ,  $L_{PO}$  and  $H$  are constants.

In related work Horn (1981) argues that digital terrain models provide convenient surface descriptions for use in the study of hill-shading for maps. They can also be used for the automatic registration of satellite images with surface models (Horn and Bachman 1978).

Shape from Shading is a practical tool in industrial situations since it is often possible to control the lighting. The reflectance characteristics of the viewed objects are also known. Techniques like photometric stereo can then be employed to find the orientation values of objects. An example is work done

by Horn, Ikeuchi et al (Ikeuchi et al 1984, Horn and Ikeuchi 1984) linking a Puma robot with a vision system which makes use of photometric stereo.

## 9. Photometric Invariants

Another branch of research tries to find what can be extracted from the intensity without explicit knowledge of the reflectance map but merely its functional form. More precisely use is made of the fact that the reflection function depends on the geometry of the surface only through the surface normal.

We first need some concepts from differential geometry (Do Carmo 1976). At every point on a surface there are two orthogonal directions in which the curvature of the surface changes most. These are called the *principal directions of curvature*. The curvatures in these two directions are *the principal curvatures*. These properties are independent of the orientation of the surface. The product of the principal curvatures is the *Gaussian curvature*, see figure 11. If the principal curvatures are of opposite sign the Gaussian curvature is negative and the surface is *hyperbolic*. An example of a hyperbolic surface is a saddle point. If the principal surfaces have the same sign the Gaussian curvature is positive and the surface is *elliptic*. Regions of positive and negative curvature will be separated by lines with zero Gaussian curvature. These are

called *parabolic lines*.

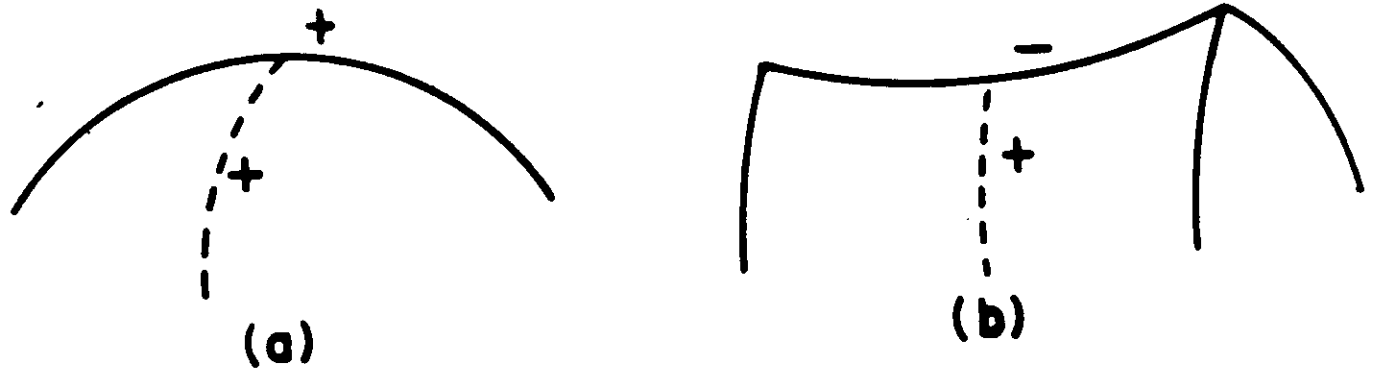
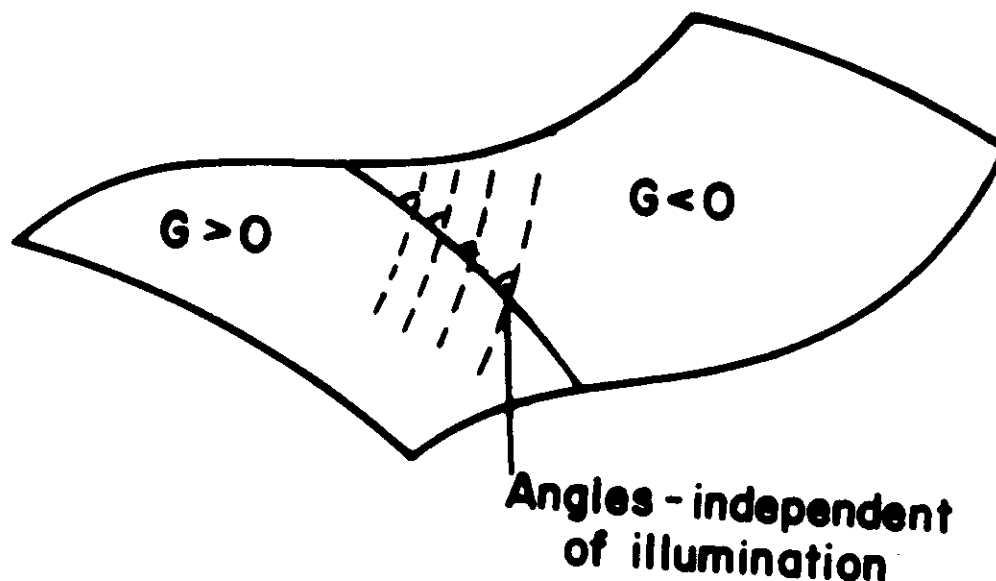


Figure 11(a) shows a surface with both principal curvatures positive and hence positive Gaussian curvature. In figure (b) the principal curvatures are of opposite sign and the Gaussian curvature is negative.

Koenderink and van Doorn (1980) investigated *photometric invariants*, features of the image that do not vary as the light source is moved. They derive relations between features in the image intensity and geometric features of the object being viewed. More precisely they consider the maxima and minima of the image intensity and show that most of them lie on parabolic lines of the underlying surface. At these points the Gaussian curvature changes sign and the surface changes from being hyperbolic to elliptic. Furthermore they show that the isophotes, the lines of constant image intensity, cut the parabolic lines



at constant angles, see figure 12. These results were re-derived and extended by Yuille (1984) who showed that at the parabolic lines the isophotes lay along the lines of curvature of the object and hence were determined by the surface geometry independent of the lighting conditions or the reflectance function. He also investigated the zero crossings of the second directional derivative and showed that they tended to lie near the extrema of curvature of the surface. It is an intriguing possibility that results of this type combined with the information available from bounding contours may be able to give a qualitative description of an object without explicit knowledge of its reflectance function.



*Figure 12. The isophotes, shown by dashed lines, cut the line of zero Gaussian curvature at constant angles independent of the reflectance function. At the intersection their tangent lie in the direction of the lines of curvature*

*of the surface.*

## 10. Computer Graphics

Present theories of shape from shading only work in restricted lighting conditions for objects with simple reflection functions and it is unlikely that they can work for general scenes. It may, however, be possible to use shading information to obtain qualitative information about objects. The reflectance models of Computer Graphics could be the basis for such a theory.

In recent years there has been considerable interest in modelling real scenes with Computer Graphics. For realistic effects the reflectance functions of objects must be modelled exactly. Films like "Tron" show how effective present techniques are.

The reflectance function concept was introduced into Computer Graphics by Phong (1975). He suggested modelling the reflectance function as a combination of Lambertian and Specular components. This is given by

$$R_p = C_p(\cos(i)(1 - d) + d) + W(i)(\cos(s))^n \quad (10.1)$$

where  $C_p$  is the reflectance coefficient of the object,  $d$  the environment diffuse reflection coefficient and  $W(i)$  is a function giving the ratio of the specular

reflected light to the incident light. Blinn (1977) introduced the lighting models of Torrance and Sparrow (1967) which modelled the surface as a set of planar facets with specular components and a diffuse component due to multiple reflections. This work was extended by Cook and Torrance (1982) who emphasized the wavelength dependence of reflectance. Intuitively an object reflects light either at the surface, in which case the reflectance is specular and the wavelength is independent of the material, or below the surface. In this case the reflected light depends on the object and can often be assumed to be Lambertian. Metals are good conductors of electricity and so the electromagnetic field of light does not penetrate them far. Thus their reflectance functions have mostly specular components.

An important effect described by these models is off-specular reflectance. This occurs when light is incident from a non normal direction. A maximum in the distribution of the reflected radiance occurs at an angle larger than the specular angle.

The Cook and Torrance model assumes that the reflectance is a sum of three components: specular, diffuse and ambient. The ambient and diffuse components reflect light in all directions equally. The specular reflectance is

$$R_s = \frac{F}{\pi} \frac{DG}{(\vec{N} \cdot \vec{L})(\vec{N} \cdot \vec{V})} \quad (10.2)$$

The geometrical attenuation factor  $G$  accounts for the shadowing and masking of one facet by another (Blinn 1977). The facet slope distribution function  $D$  represents the fraction of facets that are oriented in the direction  $\vec{H}$  (Blinn 1977). The Fresnel factor  $F$  depends on the reflectance spectra of the material and is a function of wavelength. These functions are complex and often need to be determined by experiment (see Gubreff et al 1960). In general  $F$  depends on the geometry of reflection and hence the colour varies with direction. For example for copper the colour of the reflected light approaches the colour of the light source as the incident angle approaches  $\pi/2$ .

A typical plastic has a substrate that is transparent or white, with embedded pigment particles. Thus the light reflected directly from the surface is only slightly altered in colour from the light source. This is well modelled by Phong and Blinn. The more complex model of Cook and Torrance is also suited for modelling plastics. Moreover it also produces realistic metals, unlike many computer graphics which tend to make everything seem plastic.

Many surface materials in the natural world are anisotropic, for example, cloth is a weave of threads each of which scatters light narrowly in the direction of the thread and widely in the perpendicular direction. It is relatively straightforward to generalize the Phong model to get anisotropy.

There has been comparatively little work inverting these models to get

shape, or other information. An interesting exception is the work of Shafer (1984) who proposes using colour vision to distinguish between the lambertian and specular components. He models reflectance by a combination of interface ("specular") and body ("diffuse") reflections. These have different specular behaviour and he describes a method of using colour to separate the reflection into its interface and body components. This gives a possible solution to the old vision problem of extracting the specular components of an image.

## 11. Occluding Boundary Information

It has long been known that occluding boundaries give a lot of information about the shape of objects. Picasso's picture "The Rites of Spring" gives a strong impression of shape despite the paucity of information (Marr 1977), see figure 13. Marr argued that the visual system needed to make assumptions to interpret these contours and, in particular, he proposed that the distinction between convex and concave segments reflected real properties of the viewed surface. He assumes that there are no invisible occluding edges. He claimed that these assumptions could only be satisfied if the perceived boundary rim was planar. This is a very strong assumption and recent results by Koenderink have shown it to be unnecessary. Using it Marr was able to show that if it held

for all views of an object about a given axis then the object was a generalized cylinder (Binford 1971) about that axis.



*Figure 19. The Rites of Spring*

The *boundary contour*, or *silhouette*, is the projection of the boundary onto the image plane. The points on the object which give rise to the bounding contour are called the *boundary rim*. At these points the light rays just graze the surface of the objects. If we assume orthographic projection onto a plane with surface normal  $\vec{k}$  then the equation of the boundary rim is given by

$$\vec{k} \cdot \vec{n} = 0. \quad (11.1)$$

where  $\vec{n}$  is the normal to the surface. This equation only holds for occluding boundaries where the surface turns away smoothly from the viewer. This

can be contrasted with discontinuity boundaries, for example the boundary of a sharp knife. Barrow and Tennenbaum (1981) observed that for occluding boundaries the normals at the boundaries can be easily determined. The  $x, y$  components are available directly from the image and from (9.1) we see that the  $z$  component vanishes. This result can be used to get boundary conditions for shape from shading.

Koenderink and van Doorn (1982) consider the way the projected contours of smooth objects end. They show there are a small number of rules for the way contours in the image can disappear. These results can be deduced from a more general theorem proved by Koenderink (1984). This result states that the sign of the curvature of the projected curve is equal to the sign of the Gaussian curvature of the object at the boundary rim, see figure 14. This is true for both orthographic and perspective projection. This result means that concave and convex segments on the curve do correspond to meaningful properties of the surface as Marr (1977) claimed, but that the planarity assumption is unnecessary. It is clear that contours can only end when they correspond to negative curvature of the surface. In this case the projected curve must be concave at the endpoint.

of the bounding contour. This is true for both discontinuous and occluding boundaries. An application is for *developable surfaces* for which at each point on the surface there is a straight line ruling through it along which the surface normal vector is constant. It can be used for looking at developable surfaces to obtain an estimate of the sign of the non-zero principal curvature.

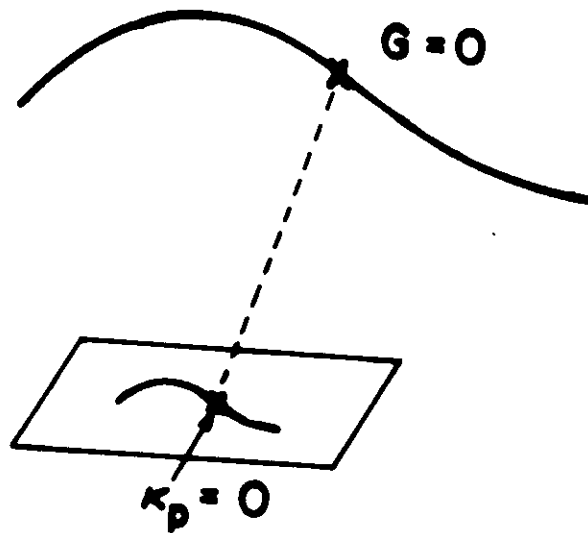
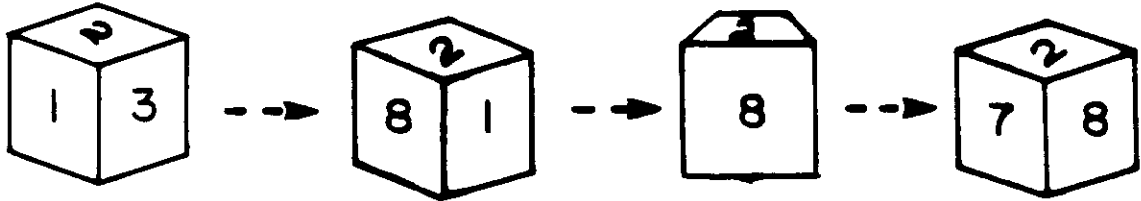


Figure 14. Points with zero Gaussian curvature,  $G = 0$ , are projected to points with  $\kappa_p = 0$ . Hence the sign of the Gaussian curvature of the boundary rim is equal to the sign of the curvature of the projected curve.

An interesting application of these results is the folding hankerchief theorem. A hankerchief is a surface which tends not expand or contract locally as it is folded. Thus its Gaussian curvature remains zero. Therefore any occluding boundary must project to a straight line in the image.



Preliminary work by Richards et al (1985) questions how we can predict what 3D objects correspond to 2D shape. They assume you are given a view of an object which they call generic; one in which all the significant events in an object which could cause occluding contours do in fact do so. This means that some objects do not have generic views. They represent surfaces by the Gaussian sphere and folds on the Gauss map correspond to the surfaces changes the sign of the Gaussian curvature. They propose rules of preference for choosing between possible ambiguous interpretations of the Gauss map.



*Figure 15. Different "frames" of a cube*

The topological structure of the silhouettes of objects change as they are viewed from different angles. For example from any given viewpoint at most three sides of a cube are visible. As the viewpoint is changed continuously we

switch to seeing three different sides, see figure 15. There are eight possible sets of three sides that can be seen at the same time. These sets correspond to the eight different *Frames* of the cube (Minsky 1975). Similarly the bounding contour of any object will vary with the orientation of the viewer. As the view-point changes cusps, convexities and concavities can appear and disappear. As these changes occur the "topology" of the silhouette alters. Koenderink and van Doorn (1985) use catastrophe theory to describe and classify these changes. With these techniques an object can be classified by the different topologies of the silhouettes it displays.

## 12. Shape from Texture

Some texture patterns can yield an extremely strong perception of depth. This effect has long been known by artists. The phenomenon was investigated by Gibson (1950) and his school and many striking demonstrations of the effect were found. Most of the theoretical analyses, however, were limited and usually restricted to texture gradients on horizontally extended planes.

Most recent work assumes that primitive texture elements can be extracted from the image. These elements are characterized by a set of parameters. These parameters can be determined from the image and put local

constraints on the surface orientation. For example the elements could be the small circular holes on a golf ball, see figure 16. In the image these holes would appear as ellipses whose size and orientation determine the local surface orientation. Once constraints on the local surface normal are known the surface itself can be constructed by interpolation. Ikeuchi (1980) described and demonstrated an algorithm of this type. It has many parallels to his work on shape from shading.

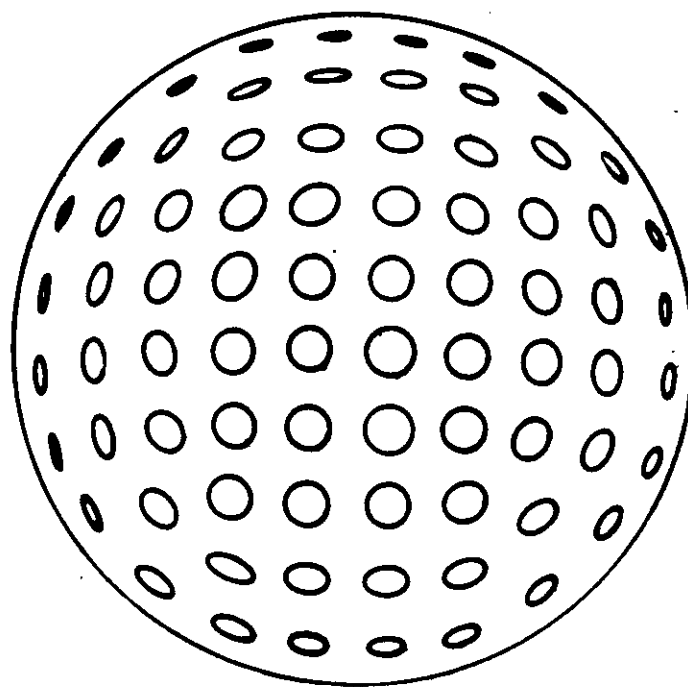


*Figure 16. The regular spacing of the holes of a golf ball give an example of shape from texture.*

Ikeuchi makes four assumptions. (1) The surface is covered with a uniform texture of repeated texture elements. (2) Each texture element is small, compared with the distance between the viewer and the viewed surface. (3)

Each texture element is small, compared with the change of surface orientation there. (4) The original shape of the texture element is known.

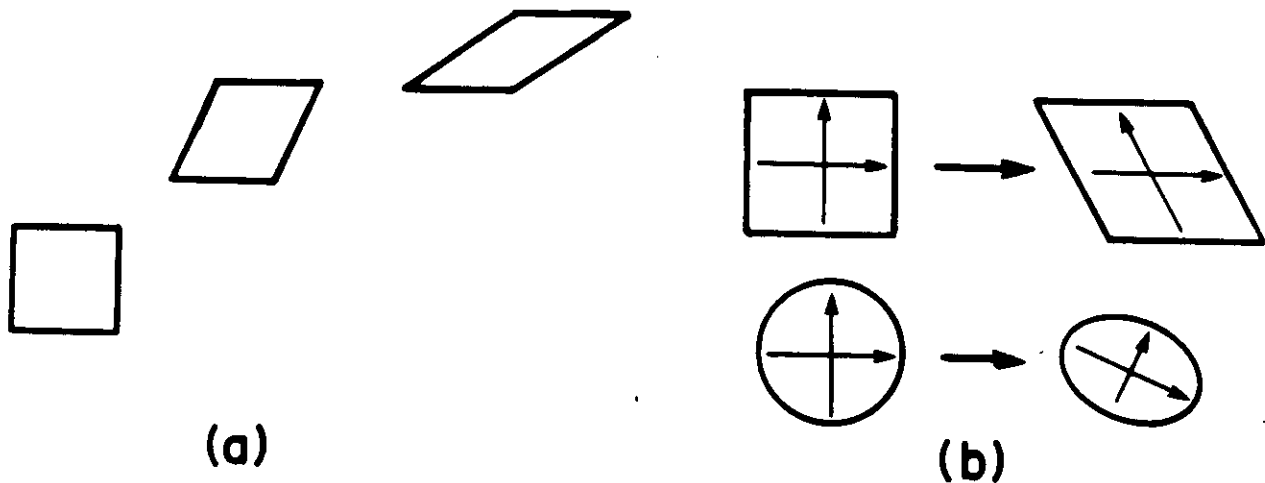


*Figure 17(a) shows the distortions of a square under projection. Figure (b) shows how projection distorts symmetry axes.*

He now defines a measure of distortion for regular patterns. Figure 17 shows the distortion of the projection of squares on a plane. This distortion depends on two factors. The first is the orientation of the surface, which is to be determined. The other is the orientation of the squares in the plane of the surface. The goal is to find an intrinsic measurement that depends only on the surface orientation. Ikeuchi argues that this can be obtained by considering the distortion of the two axis vectors, for the square these axes are perpendicular. He shows that the magnitude of the cross product of two

axis vector projections is proportional to  $\cos\omega$  and the sum of squares of their lengths is proportional to  $1 + \cos^2\omega$  where  $\omega$  is the angle between the direction of the viewer and the direction of the surface orientation. These two values are independent of the rotation angle of the regular pattern. For spherical projection, see figure 18, these two values will depend on the distance to the object, but their ratio will not. The ratio is then an intrinsic measurement as required. Ikeuchi calls this the distortion value  $I$ .

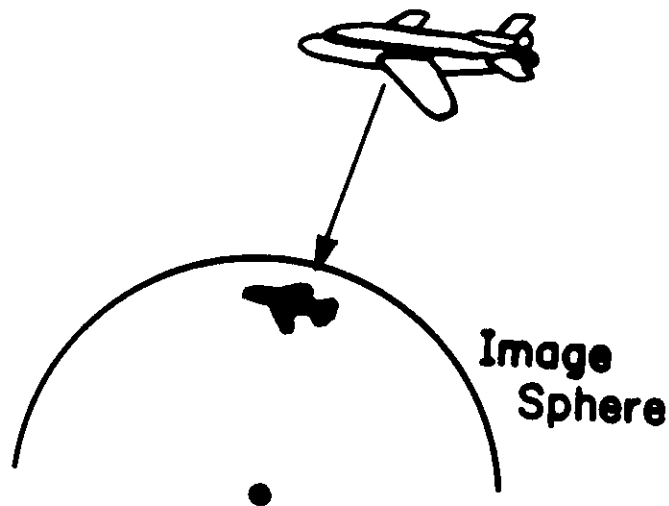


*Figure 18. The geometry of spherical projection. A point in space is projected to the unit sphere by the line joining it to the centre of the sphere.*

$$I = \frac{fg \sin\tau}{f^2 + g^2} \quad (12.1)$$

where  $f$  and  $g$  are the observed lengths of the axis vectors on the image

sphere and  $\tau$  is the angle between the two projected axis vectors. These qualities  $f$ ,  $g$  and  $\tau$  can be directly measured from the image. In terms of surfaces rotation

$$I = \frac{\cos\omega}{1 + \cos^2\omega} \quad (12.2)$$

where  $\omega$  is the angle between the direction of the viewer and the surface normal. These equations eliminate one degree of freedom of the surface, in this sense they are similar to the image irradiance equation in shape from shading. Several strategies can be used to solve for the final degree of freedom. One possibility is to take two, or more, views of the textured surface, this is roughly analogous to doing photometric stereo. Another approach is to use a smoothness constraint requiring that neighbouring points have nearly the same orientation. This is similar in spirit to the variational approach to shape from shading. Ikeuchi defines an iterative algorithm to solve the problem. This involves specifying the surface normals at the boundary and then using the smoothness constraint to propagate the solution inwards. He does not explicitly write an energy function and then minimize it, however his approach can be formulated in this way.

Kender (1980) described another method of this type. He showed that using perspective, rather than orthographic, projection yielded tighter con-

straints despite the additional complexity. He introduces a set of normalized texture property maps that provide local constraints on the surface orientation and can be thought of as a generalization of the image irradiance equation. A similar method is proposed by Ballard (1981).

An alternative model based on probabilistic concepts was developed by Witkin (1982). He suggests a model for texture formation involving isotropy and chooses the best-fit surface.

Texture can give strong cues for shape but usually only when it consists of many identical elements, or is isotropic. Most theories assume that the form of these elements is known in advance and few suggest ways of finding such elements in a natural image. Witkin's theory is an interesting exception.

### 13. Conclusion

Shape from shading, shape from occlusion and shape from texture are important vision modules and in the last few years considerable progress has been made towards understanding them. Despite their many successes it seems unlikely that, except in some limited domains, they will ever seriously rival stereo or structure from motion as sources of depth information. As yet shape from shading only works in straightforward lighting situations for objects with

simple reflectance functions while the assumptions of uniformity of texture are rarely satisfied in real images.

These modules may, however, be able to supply a lot of qualitative information about the image. It is surprising how many constraints the shape of an occluding boundary puts on a surface. It will be interesting to see if a *qualitative* theory of shape from shading can be constructed to complement these results and to further constrain the surface. Such a qualitative theory would detect significant events in the surface, for example ridges and troughs. Perhaps it will be possible to exploit the phenomenological models of Cook and Torrance (1982) to distinguish between different types of objects, such as metals and plastics, on the basis of their reflectance.

## Acknowledgements

This report describes work done within the Artificial Intelligence Laboratory at the Massachusetts Institute of Technology. Support for the A.I. Laboratory's research is provided in part by the Advanced Research Projects Agency of the Department of Defense under Office of Naval Research Contract N00014-80-C-0505.

I would like to thank A. Bobick, T. Poggio, W. Richards and S. Ull-



man for many useful discussions. I would particularly like to thank J. Little and C. Torras for critically reading the manuscript and offering many helpful suggestions.

## References

- Baddoura, J. Personal Communication. (1985).
- Ballard, D.H. "Parameter networks: Towards a theory of early vision," in *Proc. 1981 Int. Jt. Conf. Artificial Intelligence*. Vancouver, B.C. (1981).
- Barrow, H.G. and Tennenbaum, J.M. "Interpreting Line Drawings as Three dimensional surfaces," *Artif. Intell.* 17 (1981).
- Binford, T.O. "Inferring surfaces from images," in *Proc. IEEE Conf. Systems and Control*. Miami, Florida. (1971).
- Blake, A. "Specular Stereo," *Proceedings IJCAI*. Los Angeles. (1985a).
- Blake, A. Personal Communication. (1985b)
- Blinn, J. "Models of light reflection for computer synthesized pictures," *Computer Graphics* vol.11,2. (1977).
- Brady, J.M., Ponce, J., Yuille, A.L. and Asada, H. "Describing Surfaces," To appear in *Comp. Vis. Graph. and Im. Proc.* (1985).

Brooks, M.J. "Shape from Shading Discretely," Ph.D. thesis Essex University, (1982).

Brooks, M.J. and Horn, B.K.P. "Shape and Source from Shading," M.I.T. Artificial Intelligence Laboratory AI-Memo 820. (1985).

Bruss, A.R. "The Image Irradiance Equation: Its solutions and application," M.I.T., Artificial Intelligence Laboratory Technical Report, AI-TR-623. (1981).

Cook, R.L. and Torrance, K.E. "A Reflectance Model for Computer Graphics," *ACM Transactions on Graphics*. Vol.1 No.1 (1982).

Courant, R. and Hilbert, D. *Methods of Mathematical Physics*, vol. 1. Interscience Publishers, New York. (1953).

Do Carmo, M.P. "Differential geometry of curves and surfaces," Prentice-Hall, Inc. Englewood Cliffs, New Jersey. (1976).

Gibson, J.J. "This perception of the visual world," Houghton-Mifflin, Boston, Mass. (1950).

Horn, B.K.P. "Shape-from-Shading: A Method for Obtaining the Shape of a Smooth Opaque Object from one View," MAC-TR-79 and AI-TR-232, Artificial Intelligence Laboratory, M.I.T., (1970).

Horn, B.K.P. "Obtaining Shape from Shading Information," in *The Psychology of Computer Vision*, P.H.Winston, Ed., McGraw-Hill, New York.

(1975).

Horn, B.K.P. "Understanding Image Intensities," *Artif. Intell.* 8. (1977).

Horn, B.K.P. and Bachman, B.L. "Using synthetic images to register real images with surface models," *Comm. ACM*, 21 (1978).

Horn, B.K.P., Woodham, R.J. and Silver, W.M. "Determining Shape and Reflectance using Multiple Images," Artificial Intelligence Laboratory Memo 490, M.I.T. (1978).

Horn, B.K.P. "Hill-Shading and the Reflectance Map," Image Understanding Proceedings (1979).

Horn, B.K.P. and Sjoberg, R.W. "Calculating the Reflectance Map." *APPL. Opt.* 18. (1979).

Horn, B.K.P. "Sequins and Quills- Representations for surface topography," in Representations of 3-dimensional objects, R. Bajcsy, Ed., Springer-Verlag, Berlin and New York, (1982).

Horn, B.K.P. "Extended Gaussian Images," M.I.T. Artificial Intelligence Laboratory Memo 740 (1983).

Horn, B.K.P. and Ikeuchi, K. "The Mechanical Manipulation of Randomly Oriented Parts", *Scientific American* 251 (2). (1984).

Horn, B.K.P. and Brooks, M.J. "The Variational Approach to Shape from Shading," M.I.T. Artificial Intelligence Laboratory Memo 813. (1985).

Huffman, D.A., "Impossible Objects as Nonsense Sentences," *Machine Intelligence 6*, Meltzer, R., and Michie, D. (Eds), Edinburgh University Press. (1971).

Ikeuchi, K. "Shape from Regular Patterns," M.I.T. Artificial Intelligence Laboratory Memo 567. (1980).

Ikeuchi, K. and Horn, B.K.P. "Numerical shape from shading and occluding boundaries," *Artificial Intelligence. 17*. (1981).

Ikeuchi, K. "Constructing a Depth Map from Images," M.I.T. Artificial Intelligence Laboratory Memo 744. (1983).

Ikeuchi, K., Nishihara, H.K., Horn, B.K.P., Sobalvarro, P. and Nagata, S. "Determining Grasp Points using Photometric Stereo and the PRISM Binocular Stereo System," M.I.T. Artificial Intelligence Laboratory. Memo 772 (1984).

Kender, J. "Shape from texture," Tech. Rep. CMU-C5-81-102, Dept. Comp. Sci. Carnegie-Melon Univ, Pittsburgh. (1980).

Koenderink, J.J. and van Doorn, A. "Photometric invariants related to solid shape," *Optica Acta* 27. (1980).

Koenderink, J.J. and van Doorn, A. "The shape of smooth objects and the way contours end," *Perception*. 11. (1982).

Koenderink, J.J. "What tells us the contour about solid shape?" Dept.

Medical and Physiol. Physics, Univ. Utrecht, Netherlands. (1984).

Koenderink, J.J. and van Doorn, A. Preprint. Dept. Medical and Physiol. Physics, Univ. Utrecht, Netherlands. (1985).

Mackworth, A.K. "Interpreting Pictures of Polyhedral Scenes," *Artific. Intell.* 4. (1973).

Marr, D. "Analysis of occluding contour," *Proc. R. Soc. Lond.B.* (1977).

Marr, D. "Vision," W.H. Freeman and Company, U.S.A. (1982).

Minsky, M. "A framework for representing knowledge," in *The Psychology of Computer Vision.* ed. P.W. Winston. (1975).

Pentland, A. "Local shading analysis," *Pattern Analysis and Machine Intelligence.* Vol. 6. No. 2. (1984).

Phong, Bui Tuong. "Illumination for Computer Generated Pictures," *Communications of the Association for Computing Machinery, Inc.* Vol. 18, No. 6. (1975).

Richards, W. Koenderink, J.J. and Hoffman, D. "Inferring 3D shapes from 2D codons," M.I.T. Artificial Intelligence Laboratory Memo 840. (1985).

Shafer, S.A. "Using Colour to Separate Reflection Components," To appear in *Colour Research and Applications*, (1985).

Silver, W.M. "Determining shape and reflectance using multiple images," M.Sc. dissertation, A.I. Lab, M.I.T. (1980).

Sjoberg, R.W. "Atmospheric effects in satellite imaging of mountainous terrain," M.I.T., Artificial Intelligence Laboratory Technical Report, AI-TR-688. (1982).

Strat, T.M., "A Numerical Method for Shape from Shading from a Single Image," M.S. Thesis, Dept. of E.E. and C.S., M.I.T., (1979).

Todd, J.T. and Mingolla, E. "Perception of Surface Curvature and Direction of Illumination from Patterns of Shading," *Journal of Experimental Psychology: Human Perception and Performance*. Vol 9. No. 4. (1983).

Torrance, K.E. and Sparrow, E.M. "Theory for Off-Specular Reflection from Roughened Surfaces," *Journal of the Optical Society of America*. Vol. 57, No. 9. (1967).

Witkin, A. "Shape from contour," M.I.T., Artificial Intelligence Laboratory Technical Report, AI-TR-589. (1980).

Woodham, R.J. "Analyzing Images of Curved Surfaces," *Artific. Intell.* 17. (1981).

Woodham, R.J. "Photometric Stereo: A Reflectance Map Technique for Determining Surface Orientation from a Single View," *Image Understanding Systems and Industrial Applications*. Proceedings SPIE 22nd Annual Technical Symposium, Vol. 155. (1978).

Woodham, R.J. "Reflectance Map Techniques for Analyzing Surface De-

fects in Metal Casting," AI-TR-457, Cambridge, M.I.T. Artificial Intelligence Laboratory. (1978).

Woodham, R.J. "Using digital terrain data to model image formation in remote sensing," SPIE Vol. 238 Image Processing fo Missile Guidance (1980).

Woodham, R.J. and Lee, T.K. "Photometric Method for Radiometric Correction of Multispectral Scanner Data," Technical Report 84-14. Lab. Computational Vision. Dept. Comp. Sci. University of British Columbia. (1984).

Yuille, A.L. "Zero crossings on lines of curvature," M.I.T. Artificial Intelligence Laboratory Memo 718. (1984).

Yuille, A.L. and Brady, J.M. In Preparation. (1986).